environments

Article

Impact of Old Pb Mining and Metallurgical Production in Soils from the Linares Mining District (Spain)

Carlos Boente [1,*], Carlos Sierra [2], Julián Martínez [3], Eduardo Rodríguez-Valdés [4], Elías Afif [5], Javier Rey [6], Isabel Margarida Horta Ribeiro Antunes [7] and José Luis Rodríguez Gallego [4]

1 CIQSO-Center for Research in Sustainable Chemistry, Associate Unit CSIC-University of Huelva "Atmospheric Pollution", Campus El Carmen s/n, 21071 Huelva, Spain
2 Escuela Superior de Ingenieros de Minas y Energía, Campus de Vegazana, University of León, 24071 León, Spain; csief@unileon.es
3 Departamento de Ingeniería Mecánica y Minera, EPS de Linares y CEACTEMA, Universidad de Jaén, Campus Científico Tecnológico, 23700 Linares, Spain; jmartine@ujaen.es
4 INDUROT & Environmental Biogeochemistry and Raw Materials Group, University of Oviedo, C/Gonzalo Gutiérrez Quirós s/n, 33600 Mieres, Spain; rodriguezreduardo@uniovi.es (E.R.-V.); jgallego@uniovi.es (J.L.R.G.)
5 Department of Organisms and Systems Biology, University of Oviedo, Calle Cat. José María Serrano, 10, 33006 Oviedo, Spain; elias@uniovi.es
6 Departamento de Geología, EPS de Linares y CEACTEMA, Universidad de Jaén, Campus Científico Tecnológico, 23700 Linares, Spain; jrey@ujaen.es
7 Institute of Earth Sciences, ICT, Pole of University of Minho, Campus de Gualtar, 4710-057 Braga, Portugal; imantunes@dct.uminho.pt
* Correspondence: carlos.boente@dimme.uhu.es

Abstract: Mineral processing and metallurgy production centers may leave a far-reaching fingerprint of soil contamination. This scenario is particularly relevant in the mining district of Linares (Southern Spain), where former industrial sites are now dedicated to other land uses. Within this context, we selected five sectors of concern in Linares region, which are currently used as agricultural and residential areas. The study began with an edaphic characterization, including grain-size fractioning and soil chemical analyses, which were complemented by mineralogical and sequential extraction information. Anomalous soil concentrations of As, Cd, Cu, Pb, and Zn were found, with higher values than the admissible regional guideline limits. Moreover, chemical speciation indicated that in general, Pb, Zn, and Cd were highly available and bound mainly to the carbonate fraction. In addition, health risk assessment evidenced potential threats by Pb and As. Regarding remediation approaches, we observed that, in soils affected by mining and ore dressing activities, the clay and silt size fractions contained the highest pollution load, making them suitable for a size classification treatment. By contrast, in areas affected by metallurgical activity, pollutants were prone to be evenly distributed among all grain sizes, thereby complicating the implementation of such remediation strategies.

Keywords: soil pollution; heavy metals; risk assessment; remediation

check for updates

Citation: Boente, C.; Sierra, C.; Martínez, J.; Rodríguez-Valdés, E.; Afif, E.; Rey, J.; Antunes, I.M.H.R.; Gallego, J.L.R. Impact of Old Pb Mining and Metallurgical Production in Soils from the Linares Mining District (Spain). *Environments* **2022**, *9*, 24. https://doi.org/10.3390/environments9020024

Academic Editor: Paula Alvarenga

Received: 30 December 2021
Accepted: 28 January 2022
Published: 31 January 2022

Publisher's Note: MDPI stays neutral with regard to jurisdictional claims in published maps and institutional affiliations.

1. Introduction

The development of the mining and metallurgy industry over the 20th century led to a significant chemical environmental pollution (e.g., the accumulation of alkaline water, soil contamination, and dispersion and mobilization of potentially toxic elements). Many studies have revealed that the accumulation of chemicals in former mining and metallurgy sites can damage the quality of soils in the nearby areas, which leads to undesirable effects risks for living organisms [1–4]. This scenario is particularly relevant when mechanical weathering such as deflation, erosion, and thermal stress act coupled to active chemical

weathering, hydration, or hydrolysis of the silicates and carbonates [5–7], thus releasing pollutants into the environment [8].

Potentially toxic elements are among the most common toxicants affecting these sites. Comprising high-density elements with metallic properties, this imprecise category includes transition metals, semimetals, lanthanides, and actinides [9]. These compounds are characterized by their persistence (unlike other contaminants, their concentration does not decay with time) and their predisposition to bioaccumulation and biomagnification [10].

The mobility of the abovementioned metals is generally determined by precipitation, diffusion, volatilization, and dissolution of unstable minerals, in addition to other surface complexation processes [11,12]. Moreover, their bioavailability in soils and sediments may vary in function of the pH, redox potential (Eh), and organic matter content of the soils, effects that are very frequent in mining soils [13–15], as well as changes in land-use patterns [16].

The risk assessment considers both exposure and hazard and, therefore, the compound's bioavailability. It implies the use of methodologies to estimate the probability of incidence of any given magnitude causing adverse effects to health during a certain time period [17]. In this regard, baseline human health risk assessment (BHRA) is the study of the potential adverse effects on health that are caused by exposure to hazardous materials released from a place in the nonappearance of any measures that are capable of mitigating or controlling their mobility (i.e., under an assumption of no action) [17]. The Risk Assessment Guidance for Superfund [17] served as a basis to develop the BHRA model, since it is considered that simple site-specific risk assessment offers a reasonable compromise between site-specificity and effort [18].

In the case of heavy metal(loid) remediation, most strategies are based on the isolation and treatment of the polluted soil; these approaches include [19,20] the following processes: (1) physical, by concentrating pollutants into a smaller volume of soil through physical separation processes or by electrokinetic procedures that eliminate potentially toxic elements by inducing an electric current; (2) chemical, by dissolving pollutants adhered in soil particles by water washing and then treating this contaminated water with agents of solidification to produce a relatively inert cement-like material; (3) thermal, by heating the pollutants to encourage their controlled evaporation and condensation; and (4) biological procedures that use living organisms for the remediation of the soil, as is the case of phytoremediation. In all of these remediation options, it is important to assess the composition of the soil as well as the availability, mobility, and spatial distribution of the pollutants [21].

Among the abovementioned methods, physical separation is a particle separation process that removes contaminants from the soil by concentrating them into a smaller volume [21–24]. This procedure exploits differences between the characteristics of metal-bearing particles and soil particles (size, density, hydrophobic surface properties, and magnetism), in a similar procedure used on treat mineral ores [22,24]. Several parameters determine the efficiency physical separation, particle size distribution, particulate shape, clay content, humic content, heterogeneity of soil matrix, density differences between soil matrix and pollutants, and magnetic properties [25,26]. Notwithstanding, the main parameters to consider are the degree of liberation, proportion of fine particles, and the volume of soil to be treated [24]. In this regard, the degree of release indicates the percentage of a particular phase that occurs as free particles in relation to the total of that phase present in free and locked forms [27]. The latter is important because an elevated proportion of fine particles can affect the soil washing process [24]. Thus, if most of the soil is fine-grained, chemical extraction is the selected method. Finally, the treatment of a high volume of soil may justify the construction of a soil washing plant that otherwise would not be advisable owing to cost.

Moreover, phytoremediation has been widely used to degrade, assimilate, metabolize, and detoxify contaminating substances. This procedure makes use of the combined action of plants and microorganisms with the physiological and biochemical ability to absorb, retain, or degrade contaminants or transform them into less toxic forms [28,29].

The detoxification of contaminants from mine and metallurgic residues by phytoremediation is performed using at least one of two mechanisms, namely phytoextraction and phytostabilization [30]. The former involves the absorption of contaminants by the roots and subsequent translocation to the shoot biomass (stems or leaves), followed by plant harvest, while phytostabilization is a mechanism that uses the plant to develop a dense root system, which reduces the bioavailability and mobility of contaminants [31].

The main objectives of this research are:

- To evaluate the degree of pollution of the study areas (five selected sites included in the Linares mining district);
- To provide a vision into the threat that these pollutants may pose to the environment and the human health in the study site applying risk assessment methodologies;
- To discuss the selection of appropriate technologies for the remediation of the contaminated soil.

2. Materials and Methods

2.1. Study Area

Selected soil samples were collected in the Linares mining district (Jaén, South Spain). During the 19th century, this region was one of the main producers of Pb in the world [32–35]. The area has a rich underlying geology as a result of a fractured and faulted granite pluton with quartz mineralized veins containing galena (PbS), associated with sphalerite (ZnS), and chalcopyrite ($CuFeS_2$). The gangue of the ore is a mixture of composed minerals from eroded materials of the pluton, mainly sedimentary rocks with abundant amount of quartz (SiO_2), calcite ($CaCO_3$), and punctual barite ($BaSO_4$) [35–37]. The area has a semiarid Mediterranean climate with an average annual rainfall of 550 mm. In this context, low rain and wind erosion play a crucial role in the spread of pollutants.

On the basis of previous screenings of the contamination levels [38–40], as well as land use and proximity to centers of population, we studied the five following areas, each one corresponding to a surface area of 1 km^2 (Figure 1): The first set of samples was taken from a Quaternary colluvium (La Garza) (grid square 12), composed of sand, gravel, and clay from the dismantling of Triassic materials (shale and sandstones) and the granite outcropping in the vicinity. The soil is well developed, and cereals are cultivated in this area. There are signs of the former mining activity (vein of San Ignacio and tailings); the second set was taken from La Cruz Foundry (grid square 24), with a Triassic geological substrate, and without vegetation, except some Eucalyptus planted by the cast; the third group was collected from the Arrayanes vein, close to San Genaro mine (grid square 25). The underlying material is Triassic. The soil is moderately developed, and olives trees were planted in the area after the cessation of mining activities and removal of the tailings. Small dumps are present and were exploited as aggregates. The fourth set was collected in Arrayanes (grid square 38), in a Triassic substrate composed of shale and sandstones. The area is located in the vicinity of a former mineral processing plant. It is important to point out the accumulation of runoff from a close Pb slag spoil heap. The soil is moderately developed, and the vegetation in the area comprises olive trees. e) Finally, a set of samples was collected in the vicinity of Pozo Ancho's reef and mine shaft (grid square 51). The geological substrate is Triassic, and the area contains a vast amount of mine waste that was exploited as aggregate. The soil is moderately developed and currently used for growing olive trees.

At each one of these locations, a set of 5 samples from the tilled depth (0–35 cm) was collected in the four corners and in the center of the square by means of a stainless-steel shovel. In all the squares, the soil was passed 'in situ' through a 2-cm screen to remove rocks, gravel, and other large material. Thereafter, the samples were mixed to form a composite sample of about 50 kg.

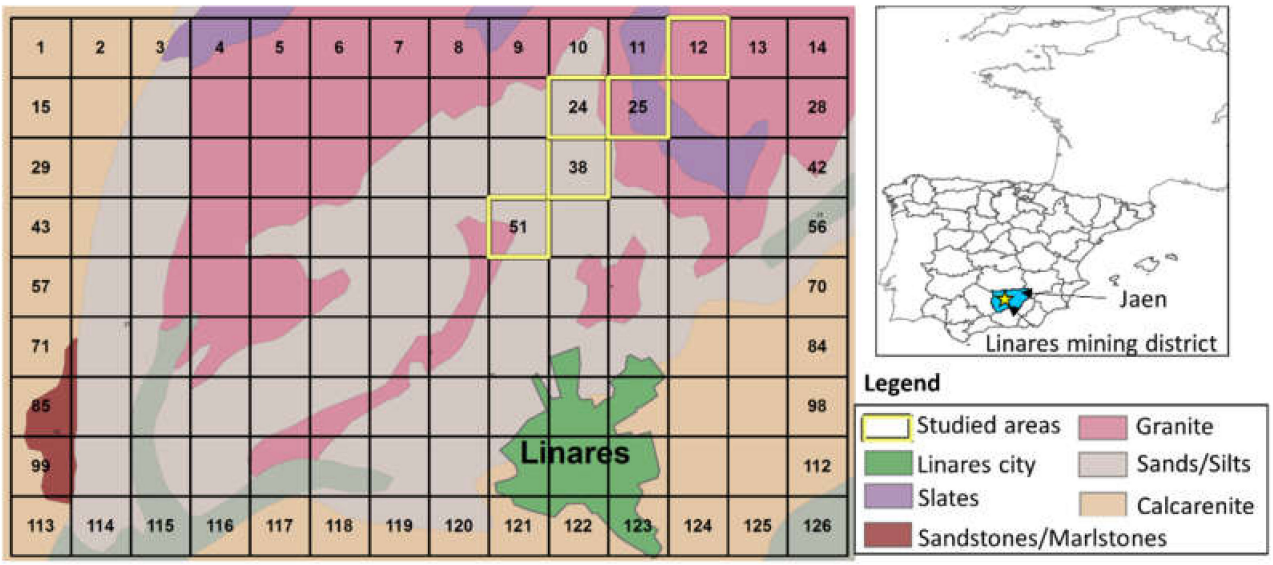

Figure 1. Situation map of the Linares mining district in the province of Jaen (Spain), with outcropping lithology and studied grid squares (1 km^2 each).

2.2. Soil Properties

Five representative soil subsamples for each of the five squares were air-dried, finely crushed, and sieved with a 2 mm screen before analysis, in duplicate. The pH was determined in a suspension of soil and water (1: 2.5) with a glass electrode, and electrical conductivity was measured in the same extract (diluted 1:5). Both analyses were carried out by means of a SevenCompact advanced benchtop pH-meter and conductivity meter (Mettler Toledo Co. Ltd.). Organic matter was measured by weight loss at 450 °C (ignition method) [41] in an OVEC-016-001 (Hobersal) laboratory oven. Total N was determined by Kjeldahl digestion [42]. The Mehlich 3 reagent [43], considered to be the most suitable extractant for a wide range of soils [44], was used to colorimetrically determine available P using a DC1500 phosphate digital colorimeter (LaMotte). Exchangeable Al was extracted with 1 M KCl and exchangeable cations (Ca, Mg, K, and Na) with 1 M NH_4Cl, and both were then analyzed by atomic absorption/emission spectrophotometry [45] in a AA200 Perkin Elmer system. The effective cation exchange capacity (ECEC) was estimated as the sum of exchangeable Al and exchangeable cations. Particle-size distribution was determined by the pipette method, after particle dispersion with sodium hexametaphosphate and sodium carbonate [46]. The composition of the silicate clay minerals (<2 μm particle-size fraction) was estimated by means of an X-ray diffractometer (Philips X Pert Pro, incorporating databases of the International Centre for Diffraction Data). In addition, representative samples were also used to prepare polished sections, which were studied under an Eclipse LV 100 POL Nikon petrographic microscope.

The representative 50-kg samples were slurried in water and then wet-sieved (cycles of 100 g) into particle-size fractions of <63, 63–125, 125–250, 250–500, 500–1000, and 1000–2000 μm using normalized sieves placed in a shaker and following the Standard Test Method for Particle-Size Analysis of Soils (ASTM D-422-63). Larger fractions were not considered because comminution is usually required for their treatment [27]. The fractions were recovered, dried at 50 °C, and finally weighed in order to construct a granulometric curve. Representative samples of each grain-size fraction were subjected to chemical analyses, although some of them were subdivided to obtain further samples for the mineralogical study.

The geoaccumulation index (Igeo) [47]: $Igeo = \log_2(C_n/1.5B_n)$, wherein C_n is the total concentration of metals in the finer soil/sediment fraction (<63 μm) and B_n are the background levels [38,40], was used to assess the pollution levels.

2.3. Sequential Extraction

A modified BCR sequential extraction procedure [48] was used to obtain four fractions. In brief, extracts with reagents of increasing strengths were attained from subsamples for 1 g for the five types of soil sample. The following fractions were obtained: carbonate-bound (extracted in a buffer of CH_3COONa/CH_3COOH; 40 mL of 0.11 mol L^{-1}); Fe-Mn oxide-bound (extracted in $NH_2OH{\cdot}HCl$; 40 mL of 0.5 mol L^{-1}); organic matter-bound (extracted in several steps using H_2O_2 (10 mL of 8.8 mol L^{-1}), and minor reductions with HNO_3 and NH_4NO_3); and residual fraction (extracted in aqua regia, following the ISO 11466 [49]). All the liquid fractions were analyzed for heavy metal (loid) content by means of ICP-OES (see Section 2.4). More detailed information about the process and specifications of titers and concentrations of reagents can be found in [50]. Although controversial as far as assessing the exact As portioning, this kind of procedures can be considered adequate for the estimation of the most easily mobilizable As [51].

The individual contamination factors (ICF) were obtained as the quotient between the sum of the nonresidual fractions (F1 + F2 + F3) and the residual fraction (F4), for each sample. Moreover, the global contamination factor (GCF) was obtained as the sum of individual ICFs for each element in a given sample [52].

2.4. ICP-OES Analysis

For the characterization of the soils, approximately 10 g of each sample was ground at 400 rpm for 40 s to a particle size < 125 µm using a vibratory disc mill (RS 100 Retsch). Next, 1 g of the milled sample was subjected to an 'Aqua regia' digestion ($HCl + HNO_3$) and finally analyzed by ICP-OES at the accredited (ISO 9002) Acme Analytical Laboratories Ltd. (Vancouver, BC, Canada) in order to determine the concentration of major, minor, and trace elements.

For the characterization of the BCR leachates, samples ranging between 1 and 5 mL were collected during the different leaching procedures and vacuum-filtered on Whatman 934-AH membranes and then acidified. Finally, the metal concentrations were measured also by ICP-OES.

2.5. Risk Assessment

BHRA for onsite receptors was conducted for As, Cd, Cu, Pb, and Zn. According to Spanish law [53], regulatory limits for metals, termed Generic Reference Values (GRV), vary depending on the land use (industrial, residential, and natural-soil) and can be considered trigger values. This means that, when they are exceeded, site-specific risk assessment is required; thus, different exposure routes associated with each use need to be considered.

In this regard, a risk characterization was performed combining toxicity assessment and exposure assessment, both considered separately for carcinogenic and noncarcinogenic effects. For carcinogenic risks, the nonthreshold assumption was adopted, and the trigger soil screening level (GRV in Spain) was set at the probability of cancer exceeding 10^{-5}. Otherwise, for noncarcinogenic compounds, the risk was considered admissible when the ratio between the long-term exposure dose and the maximum admissible dose was lower than 1 [54]. The concentrations used for the BHRA corresponded to the exchangeable fractions from the BCR sequential extraction procedure. This fraction is regarded as bioavailable or interchangeable, which means that metals are bioaccessible by plants, being taken up from the environment via cellular membranes [55]. This assumption was made considering a model definition for natural-soil land use, which states that risks related to consumption of crops grown in the potentially polluted soils can be calculated.

Thereafter, exposure assessment was performed, and parameters for frequency and duration of exposure, and pathways by which humans are potentially exposed were defined [17]. Due to lack of site-specific data, default exposure parameters presented in USEPA guidelines for Developing Soil Screening Levels and Risk Assessment [18] were considered for BHRA calculations. Additionally, values used for toxicity assessment

were taken from the Integrated Risk Information System (IRIS), following the US EPA recommendations as source of choice.

Given that there is no consensus on inorganic Pb toxicity values, it was not possible to conduct a Pb BHRA, as proposed above for the other potentially toxic elements. Therefore, this metal was considered as a special case. In this context, US EPA developed special guidelines for risk assessment of residential soil contaminated with Pb [56].

3. Results and Discussion

3.1. Edaphic and Mineralogical Soil Characterization

We performed an exhaustive edaphic characterization, the results of which are summarized in Table 1. Accordingly, the soils in the study area were slightly acid (square 24, pH = 6.87), slightly alkaline (square 12, 25, and 51, pH = 7.46, 7.50, and 7.97, respectively) or medium alkaline (square 38, pH = 8.17). The upper horizon showed low organic matter content (<1.5%). Electrical conductivity was low in samples 12, 25, and 51 (EC < 0.15 dS m^{-1}), while the square 24 and 38 had higher electrical conductivity (EC = 1.33 and 0.91 dS m^{-1}, respectively), indicating salinization issues. Salinity can have a major effect on soil structure. In this regard, soil structure, or the arrangement of soil particles, greatly affects permeability and infiltration. Soil EC can serve as a proxy for soil chemical properties such as organic matter, clay content, and cation-exchange capacity [56]. These properties have a significant effect on water- and nutrient-holding capacity, which are the major drivers of yield.

Table 1. General soil properties for the composite sample.

Soil Property	Square				
	12	**24**	**25**	**38**	**51**
Organic matter (%)	0.95	1.00	1.32	0.74	0.72
Total N (%)	0.24	0.26	0.19	0.17	0.21
C/N	2.27	2.27	3.95	2.52	2.01
pH (water 1:2.5)	7.46	6.87	7.50	8.17	7.97
Electrical conductivity (dS m^{-1})	0.03	1.33	0.14	0.91	0.06
Available P Mehlich 3 (mg kg^{-1})	2.82	1.61	1.27	7.69	2.94
Extractable K ($cmol_c$ kg^{-1})	0.24	0.29	0.32	0.81	0.22
Extractable Ca ($cmol_c$ kg^{-1})	6.12	6.28	8.48	21.27	6.54
Extractable Mg ($cmol_c$ kg^{-1})	1.18	1.21	1.15	2.97	2.35
Extractable Na ($cmol_c$ kg^{-1})	6.70	3.58	7.54	10.29	9.11
Extractable Al ($cmol_c$ kg^{-1})	0.10	0.15	0.05	0.02	0.09
ECEC ($cmol_c$ kg^{-1})	14.33	11.50	17.53	35.34	18.30

All the soil samples had a regular content of total N, between 0.17% and 0.26%, and very low C/N ratio, as expected for the low content of organic matter in these soils. Given that the critical level of Mehlich-3 available P is 30 mg kg^{-1} [44], the available P extracted with Mehlich 3 reagent was considered low in all samples (PM3 < 8.0 mg kg^{-1}).

The exchangeable base cations and the effective cation exchange capacity were moderate to low in all the analyzed soils, except sample 38, where extractable Ca and effective cation exchange capacity were higher (21.27 and 35.34 cmol(+) kg^{-1} for extractable Ca and ECEC, respectively), which were attributable to their content of clay mineral and soil pH. The cation exchange capacity of a soil generally increases with soil pH. This is because a greater negative charge develops in organic matter and clay minerals, such as kaolinite, due to the deprotonation of functional groups as pH increases. The rate of ion exchange in soils is dependent on the type and amount of inorganic and organic components and the charge and radius of the ion being considered [57]. With clay minerals such as kaolinite, where only external exchange sites are present, the rate of ion exchange is rapid. With 2:1 clay minerals that contain both external and internal exchange sites, particularly with vermiculite which has partially collapsed interlayer space sites, the kinetics are slower. In these types of clays, ions such as K^+ slowly diffuse into the partially collapsed interlayer spaces, and the exchange can be slow. The mineral soil texture in samples 24, 25, and 38 was

sandy loam, whereas square 51 was sandy, and square 12 comprised loamy sand. Therefore the particle-size soil distribution revealed a high percentage of sand fractions.

The mineralogical analyses obtained by X-ray diffraction indicated the presence of the following mineral phases: quartz, feldspar, illite, calcium carbonate, and trioctahedral vermiculite. The clay fractions were dominated by illite and trioctahedral vermiculite (2:1 clay mineralogy) in samples 12 and 25, while illite was predominant in the rest of the samples.

In addition, microscopic observations (Figure 2) were performed to determine the presence of mineral phases with potential to release heavy metals and thus susceptible to treatment with physical separation procedures. We detected the presence of hematite, magnetite, chalcopyrite, pyrite, sphalerite galena, and cerussite, as well as some slag fragments (amorphous materials resulting from the metallurgical activities) mixed with the soil.

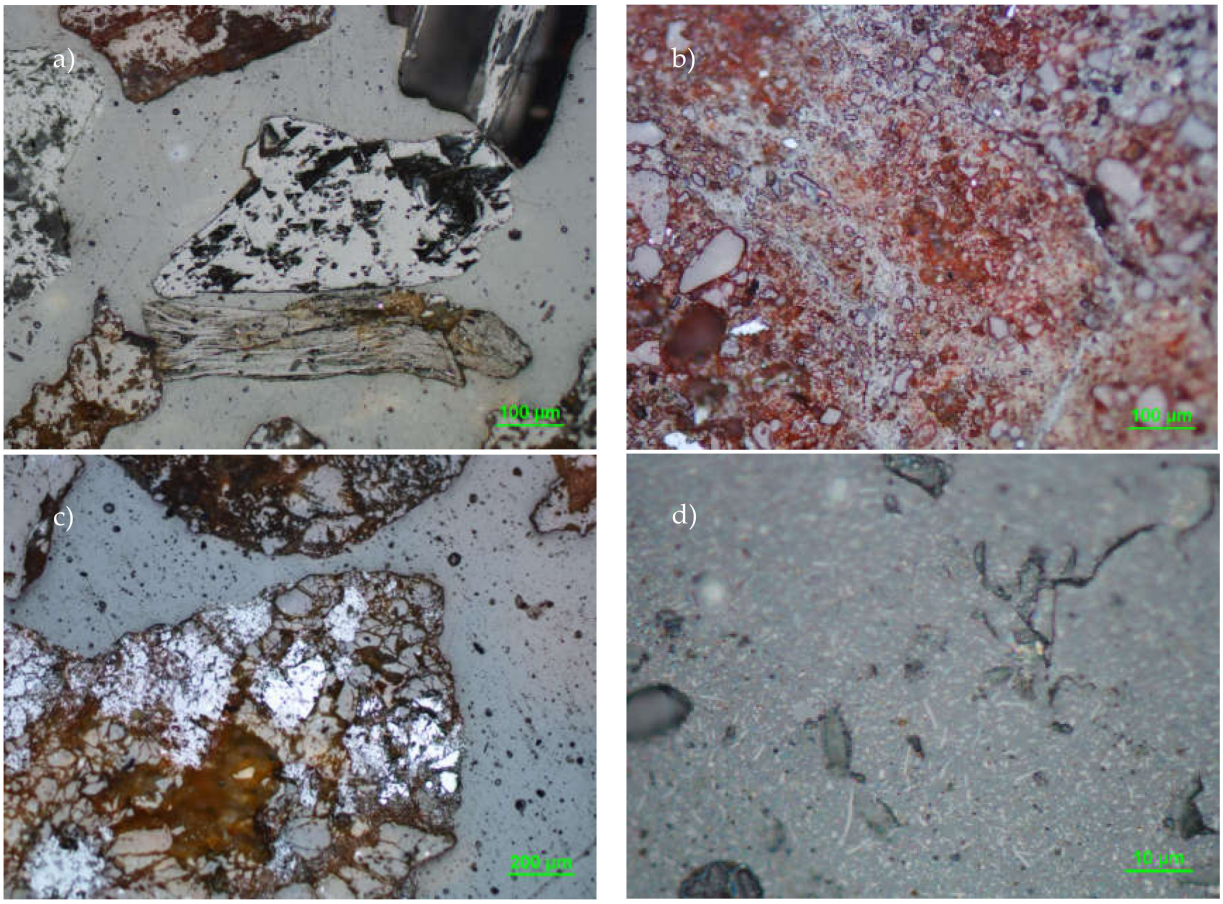

Figure 2. Light photomicrographs of some of the minerals present in the soil samples. (**a**) Galena (sometimes this mineral is partially replaced by cerussite), (**b**) hematite disseminations (average grain size from 10 to 20 µm) which are commonly found in small particles associated with metamorphic fragments, (**c**) pyrite (also this mineral is frequently partially replaced by cerussite), and (**d**) rutile disseminations in the form of altered needles (10 µm in length).

In this regard, an estimated liberation degree study allowed us to establish the threshold above which physical separation cannot be performed without milling. In this respect, and taking into consideration the heterogeneity of the soil locations and minerals, we determined that the liberation size (size below which the mineral grains are not mineral inclusions in other mineral phases) was 200 µm.

3.2. Geochemical Soil Composition and Assessment of Pollution Levels

Metal contents were compared with the average Clarke value, the mean values for acidic rocks [58–60], and the limit values set out in the legislation of the Autonomous Community of Andalusia [40] (Table 2).

Table 2. Abundances of elements of environmental concern, Clarke value, mean concentration value for acidic rocks, background values and legal values: maximum permissible and compulsory treatment values according to the legislation of the Autonomous Community of Andalusia for agricultural soils of the five squares studied. Note that in squares 12 and 24, background corresponds to granite substrate whereas for 25, 38, and 51, background levels correspond to the Triassic substrate.

		Element Concentration (mg kg^{-1})				
		As	**Cd**	**Cu**	**Pb**	**Zn**
Square	12	18.5	0.7	67	5158	33
	24	139.5	18.7	357	4244	694
	25	84.8	3.4	381	35899	473
	38	134.5	2.8	587	9872	7468
	51	41.6	1.8	722	9870	143
Reference value	Clarke	5	0.15	70	16	132
	Acid rocks	1.5	0.1	30	2	60
	Background granite	18.5	0.2	34	1149	98
	Background Triassic	18	0,2	68	1442	64
	Maximum permissible	<20	<2	<50	<100	<200
	Intervention value	>50	>7	>300	>300	>600

More specifically, As soil concentration was high in squares 24 and 38 and relatively high in square 25. Concerning Cd, similar concentrations were observed in the different sampling areas, although the mean concentration in square 24 was extremely high and clearly exceeded the values in other squares. High Cu soil concentration, a common metal in all the sampling areas except square 12, can be attributed directly to the atmospheric transport and mineralization of smoke from the smelter chimneys. Along the same lines, Pb soil concentrations were very high in all the areas, reaching values considered toxic to plants [61] and above admissible values established by law. As regards, Zn soil concentrations, the highest values, corresponded to square 38.

Moreover, an exhaustive characterization was conducted in order to facilitate the study of the relation between contaminant contents and grain-size fractions. Regarding this, the highest contents of trace elements were found in the fine fractions, 125–63 µm, and particularly below 63 µm. This observation allowed us to estimate that around 50% of the metals were present in the fraction below 125 µm (Table 3). These results are further discussed in Section 3.5.

To assess the degree of pollution, simple comparison with local background, particularly in case that concentration of polluting elements in the background is extremely high, may cause misleading interpretations. These local high concentrations may occur due to natural reasons (e.g., geological enrichments) or to anthropogenic activity (e.g., earth moving in mining, low-but-permanent release of pollutants due to industrial activities, etc.). This issue has even led to a problematic when establishing threshold levels of pollution for specific regions [62–66], thus being a topic that deserves especial consideration.

In the case of the soils in the Linares mining district, as other studies have revealed, the area is enriched by its own geology [38,40]. Thus, discerning between pollution and natural enrichment might also be difficult. A common tool to cope with this issue is to consider pollution indices, which consider a background of reference that must be previously defined. For this work, the selected index was the Igeo, which was calculated with respect to both the Clarke [59], and the local background [58] values (Table 3). The Igeo index distinguishes seven grade classes: Igeo $\leq$ 0 (grade 0), unpolluted; 0 < Igeo $\leq$ 1 (grade 1), unpolluted to

moderately polluted; 1 < Igeo ≤ 2 (grade 2), moderately polluted; 2 < Igeo ≤ 3 (grade 3), moderately to strongly polluted; 3 < Igeo ≤ 4 (grade 4), strongly polluted; 4 < Igeo ≤ 5 (grade 5), strongly to extremely polluted; Igeo > 5 (grade 6), extremely polluted.

Table 3. Particle-size distribution, element concentration in each fraction, and Igeo for each study site. Igeo was calculated according to the Clarke and the local background.

Zone	Particle Size (μm)	Wt %	Concentration (mg kg^{-1})					$I_{geo\ (Clarke)}$					$I_{geo\ (background)}$				
			As	Cd	Cu	Pb	Zn	As	Cd	Cu	Pb	Zn	As	Cd	Cu	Pb	Zn
12	2000–1000	20.69	26	0.3	32.2	2220	16	3.3	2.4	1.8	9.8	-0.5	1.4	2	2.8	3.6	0
	1000–500	24.14	12	0.4	49	4430	21										
	500–250	18.97	24	0.3	71.4	5759	30										
	250–125	10.34	19	0.4	102.2	7487	48										
	125–63	6.90	30	0.8	159.6	10481	67										
	<63	3.45	74	1.2	362.6	20963	144										
24	2000–1000	16.13	56	13.1	189.3	1665	414	6.1	7.1	3.3	9.4	2.6	4.2	6.7	4.3	3.2	3
	1000–500	16.13	65	12.7	249.3	3323	589										
	500–250	17.74	108	21.8	341.3	4319	795										
	250–125	12.90	196	19.6	487.3	5615	800										
	125–63	8.06	269	26.1	598	7861	1032										
	<63	12.90	503	31.4	1020	15722	1174										
25	2000–1000	13.11	65	2.9	267	21645	302	5	4.8	3.5	12.2	2.5	3.2	4.4	3.6	5.7	3.6
	1000–500	14.75	77	3.3	226	27056	428										
	500–250	14.75	77	3.3	292	35173	550										
	250–125	14.75	90	3.3	405	45725	659										
	125–63	11.48	149	4.8	834	64015	813										
	<63	6.56	246	6.5	1210	115227	1149										
38	2000–1000	21.67	214	7	188	14513	10080	5	4.6	1.7	9.8	7.3	3.2	4.2	1.8	3.3	8.4
	1000–500	25.00	168	5.1	133	11610	9450										
	500–250	18.33	63	2	52	6995	6300										
	250–125	13.33	43	1.5	42	5805	5760										
	125–63	3.33	78	3	76	19586	10890										
	<63	1.67	249	5.4	346	20985	32040										
51	2000–1000	12.96	28	0.4	93	6760	96	4.1	1.8	2.4	10.3	0.7	2.2	1.4	2.5	3.8	1.8
	1000–500	14.81	36	0.5	87	7970	178										
	500–250	20.37	48	0.5	108	8230	166										
	250–125	14.81	64	0.6	108	10990	216										
	125–63	11.11	56	0.5	177	17584	234										
	<63	5.56	128	0.8	568	30772	330										

Thus, with respect to the Clarke, the index revealed that soil from square 24 is extremely polluted in As (grade 6 pollution level), whereas the rest squares soils were at least strongly polluted (grade 4 or more) for the same potentially toxic element. Regarding Cd soil contents, squares 51 and 12 were moderately and severely polluted, respectively, and the rest ranged from strongly to extremely polluted (square 25, 38) to extremely polluted (square 24). Accordingly for Cu, squares 12 and 38 were moderately polluted while the rest were moderately to strongly (square 51) to strongly polluted (squares 24, 25). Regarding Zn, squares 12 and 51 were unpolluted, squares 24 and 25 moderately to strongly polluted, and square 38 extremely polluted. The Igeo presented comparable results for both local background and Clarke values, with the clear exception of Pb is which case they lowered down the pollution levels from extremely to strongly polluted.

3.3. Sequential Extraction

Results from this procedure were grouped into four main fractions (Table 4), namely carbonates (bioavailable) (F1), Fe-Mn oxyhydroxides (labile) (F2), organic matter—sulfides (immobile) (F3), and residue silicates (refractory) (F4). Individual pollution levels for contamination factor (ICF), can be interpreted as: low (ICF < 0 and GCF < 6), moderate

(1 < ICF < 3 and 6 < GCF < 12), considerable (3 < ICF < 6 and 12 < GC < 24), and high (ICF > 6 and GCF > 24).

Table 4. Percentages of the four main fractions: bioavailable (F1), labile (F2), immobile (F3), and refractory (F4) and individual contamination factors (ICF). Note that Cd results for squares 12 and 51 were not significant as the low initial concentration of this metal is closed to detection limits (DL).

	Square		**12**	**24**	**25**	**38**	**51**
Element (%)	As	F1	1.2	2	0	19.2	0.4
		F2	45.3	44.1	25.2	24.7	10.9
		F3	2.3	1.1	0	2.4	2
		F4	51.2	52.8	74.8	53.6	86.7
		ICF	0.95	0.89	0.34	0.86	0.15
	Cd	F1	<DL	58.3	51.2	21.2	<DL
		F2	<DL	21.1	19.5	27.3	<DL
		F3	<DL	4	7.3	9.1	<DL
		F4	<DL	16.6	22	42.4	<DL
		ICF	-	5.02	3.55	1.36	-
	Cu	F1	20.6	24.1	18.5	0	12.5
		F2	18.8	26.8	26.6	21	21
		F3	20.7	20.2	15.3	58.8	16.2
		F4	39.9	28.9	39.6	20.3	50.4
		ICF	1.51	2.46	1.53	3.93	0.99
	Pb	F1	66.1	46	40.8	35.6	35.5
		F2	26.6	29	51.9	48.3	48.1
		F3	3.4	16.6	3.8	7.9	7.9
		F4	3.9	8.4	3.5	8.2	8.5
		ICF	24.64	10.9	27.57	11.2	10.76
	Zn	F1	22.6	51.2	15.8	44.9	13.9
		F2	14.7	29.7	29.7	41.7	17.7
		F3	16.9	9.8	13	7.1	5.6
		F4	45.8	9.3	41.5	6.4	62.7
		ICF	1.18	9.75	1.41	14.64	0.59
	GCF		28.3	24	30.8	30.6	12.5

The first fraction (F1) exchangeable and/or associated with carbonates is considered to have the weakest bonded metals. Equilibrium for metals of this fraction is even possible with the aqueous phase. Therefore, they present high relative mobility, thus being easily bioavailable [67]. In general, Cd, Cu, Pb, and Zn soil contents, as opposed to As, were highly available as they were present in the carbonate fraction. The high concentration of these elements in this fraction may be indicative of anthropogenic contamination. This result, when interpreted according to the risk assessment code (RAC) [68], indicates that a significant number of grid squares pose a high and very high risk for the aquatic environment.

In the second fraction (F2), metals exist as cement, and/or nodules and/or concretions bond to Fe and Mn oxyhydroxides. Metals in this fraction tend to be stable under oxidizing conditions, but low Eh tends to increase their availability [68]. In our case, it was observed that this fraction acted as an important scavenger for all the studied metals but particularly for As and Pb.

The third fraction (F3) represents the amount of trace elements that are strongly bound to various forms of organic matter (organic coatings on inorganic particles including biotic detritus) [69]. Generally, this fraction is not available because of the strong interaction between the organic matter and the pollutant [67]. However, if the organic matter is destroyed, for example under strong oxidizing conditions, pollutants can be released [68]. In the analyzed soil samples, only Cu played a major role in this fraction.

Finally, the forth fraction (F4) comprises the metals incorporated into the crystal structure of the minerals. These elements do not participate in most chemical reactions

(inert) and therefore are not biologically available [69]. The element soil concentration is this fraction is high and represents natural sources, such as chemical weathering of parental rocks [68]. In this study, Pb soil concentration in F4 was low, and thus, this highlights the anthropogenic origin of most of the Pb present in the soil samples. For As, the opposite occurs; therefore, its mobility was limited.

Moreover, the ICFs and GCFs (Table 4) were used to indicate the risk of an element to the environment on the basis of its retention time (a low retention time is indicative of a greater threat). This interpretation allowed one to identify the soil squares 25 and 38 with the greatest hazard. These results highlight the importance of the most available fractions in the soil samples, which were used for the risk assessment described in the next section.

3.4. Risk Assessment

The critical values of risk characterization were derived for both carcinogenic (denoted here as CR) and noncarcinogenic compounds (HQ) for the different land uses considered in regional Spanish legislation (Table 5).

Table 5. Critical values of the risk characterization for carcinogenic (CR) and noncarcinogenic compounds (HQ) for various land uses. In bold: values exceeding risk limit for carcinogenic substances (Risk =10^{-5} and noncarcinogenic substances hazard quotient (HQ = 1).

	Industrial Scenario				Residential/Recreational				Natural Soil (Agricultural Use)			
	CR		HQ		CR		HQ		CR		HQ	
Square	As	Cd	Cu	Zn	As	Cd	Cu	Zn	As	Cd	Cu	Zn
12	$\mathbf{1.19 \times 10^{-5}}$	8.31×10^{-4}	1.68×10^{-3}	1.11×10^{-4}	$\mathbf{3.01 \times 10^{-5}}$	1.00×10^{-2}	2.21×10^{-2}	1.45×10^{-3}	$\mathbf{6.54 \times 10^{-4}}$	4.80×10^{-3}	4.27×10^{-1}	1.80×10^{-2}
24	$\mathbf{3.64 \times 10^{-5}}$	1.40×10^{-2}	4.94×10^{-3}	1.28×10^{-3}	$\mathbf{2.27 \times 10^{-5}}$	2.67×10^{-2}	1.17×10^{-2}	3.04×10^{-3}	$\mathbf{4.93 \times 10^{-3}}$	**7.58**	**3.01**	7.79×10^{-1}
25	$\mathbf{2.21 \times 10^{-5}}$	2.54×10^{-3}	5.28×10^{-3}	8.72×10^{-4}	$\mathbf{1.38 \times 10^{-4}}$	4.86×10^{-2}	1.25×10^{-1}	2.07×10^{-2}	$\mathbf{3.00 \times 10^{-3}}$	**1.56**	**2.33**	1.73×10^{-1}
38	$\mathbf{3.51 \times 10^{-5}}$	2.09×10^{-3}	8.12×10^{-3}	1.38×10^{-2}	$\mathbf{2.19 \times 10^{-4}}$	4.00×10^{-2}	1.93×10^{-1}	3.27×10^{-1}	$\mathbf{4.75 \times 10^{-3}}$	5.30×10^{-1}	9.27×10^{-2}	1.57×10^{-1}
51	$\mathbf{1.09 \times 10^{-5}}$	1.35×10^{-3}	1.00×10^{-2}	2.63×10^{-4}	$\mathbf{6.78 \times 10^{-5}}$	2.57×10^{-2}	2.37×10^{-1}	6.25×10^{-3}	$\mathbf{1.47 \times 10^{-3}}$	1.23×10^{-2}	**3.40**	4.46×10^{-2}

The risk assessment survey pointed only to As as an element of concern for industrial and residential land uses due to its carcinogenic nature. Risk values for this compound exceeded the admissible risk limit (10^{-5}) in all cases, which ranged from 1.09×10^{-5} to 2.19×10^{-4} for minimum and maximum risk, respectively. Considering described land uses, no other associated risk was identified for the compounds analyzed.

The assessment of natural-soil land use introduces As, as in other scenarios, as the element with the largest contribution to overall risk because of its carcinogenic nature. Nevertheless, Cu and Cd also exceeded the maximum accepted risk quotient (HQ = 1) for soil squares 24, 25, and 51. Four exposure pathways were considered for this type of land use, as stated by national legislation; i.e., oral ingestion (dust and soil particles), dermal contact, inhalation (vapor and soil particles), and food consumption (cultivation in polluted soils). For the latter, the soil concentrations of heavy metals used for the calculation correspond to the exchangeable fractions from the BCR sequential extraction procedure. Therefore, squares in which the mentioned fraction is not highly relevant are favored in the risk assessment calculations as metal(loid)s are less bioavailable to plants, and therefore, this exposure pathway is less important as a risk enhancer.

Since Pb is the main pollutant, the risk assessment for soil for this element was calculated following a different approach. As a conclusion, Pb soil concentrations in the grids were so high that specific risk assessment showed an unacceptable risk for human health. Inorganic Pb risk assessment was based on predicting PbBs for current and potential future populations in relation to compound exposure. All soil grids showed PbBs exceeding the limit of 5 µg/dL for both models; i.e., the adult lead methodology (ALM) for the industrial scenario, and the integrated exposure uptake biokinetic (IEUBK) model for residential use. We therefore conclude that the potential health risk is unacceptable.

This case of unacceptable risk is not an exception. In this regard, other studies worldwide that used the ALM and the IEUBK models also reported similar levels of risk near a lead–zinc mine in China [70]. However, industry related to Pb has also caused similar risks in urban street dusts at several cities around the United Kingdom [71] and even in drinking

waters of the United States of America [72], thus evidencing a need in remediating soils affected by this sort of mining and industry.

3.5. Soil Washing and Phytoremediation Options

The choice of the remediation technology varies depending on the nature, concentration of the pollutants, and on the characteristics of the soil. On the basis of the exhaustive characterization of the soil performed in the preceding sections, some comments can be performed as regards treatment options.

Isolation is neither possible nor advisable due to the amount of polluted soil; however, stabilization, which includes the use of products such as phosphorous and organic compounds, limes, and metal oxides, is feasible. In this respect, stabilization with lime, red mud (RM), and gravel sludge + red mud (GS + RM) has been successfully used in similar mining sites [73].

The stabilization using plants, namely phytostabilization, can be used in the area through the use of drought-, salt-, and metal-tolerant plants after appropriate organic amendment and irrigation of the soil [74,75]. The use of the halophyte *Atriplex* (*Chenopodiaceae* family), particularly *Atriplex lentiformis* (Torr.), as well as *S. Wats*. (quailbush), for the revegetation of the Pb/Zn polluted soils may offer an interesting alternative, which could be deducted from studies conducted in similar conditions in Australia [76].

Concerning phytoextraction, this approach would have limited application in the zone due to the lack of water and organic matter, in addition to metal(loid)s toxicity, low nutrients, and acid pH of the soils. The introduction of *Cichorium intybus* L. (chicory, *Asteraceae*) and *Cynodon dactylon* (L.) *Pers.* (bermudagrass, *Poaceae*), which naturally colonize mine tailings in Spain in similar environments, emerges as a good alternative [77]. Thus, Del Rio-Celestino et al. [78] examined Pb accumulation in two plants, reporting shoot Pb accumulation of 800–1500 and 400–1200 mg kg^{-1} Pb for *C. intybus* and *C. dactylon*, respectively, without inhibiting plant growth or biomass production. In addition, for grid square 24 soil, which has a slightly acid pH, metal accumulation using the grass *Lygeum spartum* L. (albardine, *Poaceae*), which is known on colonize acidic mine tailings site in Mediterranean regions, would be a suitable alternative, particularly for Zn [79,80].

As regards remediation, we do not recommend chemical soil washing procedures for this particular case, again because of the amount of the soil to be treated, the cost, and the environmental inconvenience of leachate processing. Nevertheless, the detailed study of both the particle-size distribution and pollution levels of each of these fractions supports physical soil washing as a feasible technique. This method would be appropriate because most of the pollutants are concentrated in the fine fraction, and the percentage of these fractions is not very high (>25%), thus facilitating volume reduction and the efficiency of the separation [22,24].

Therefore, physical soil washing by classification emerges as one of the most appropriate methods for the treatment of these soils. Thus, for grid squares 12 and 51, the removal of the fine fraction by soil-washing and its subsequent replacement by Miocene marls (a practice commonly used by farmers in the area to correct the Triassic soils) could significantly reduce the concentration of pollutants in the soil, particularly in square sample 51 considering the smaller proportion of fine particles (Table 2).

However, classification falls short, and other soil washing procedures, such as gravity concentration, would be required to improve the performance of the process. In general, gravity would appear to be feasible in all grid samples owing to the differential density between the contaminants (metallic minerals enriched in Pb) and soil aggregates. Note also that for medium grain-sizes most clean particles appear to be released (see Section 3.2) from the metal-bearing phases. Moreover, many of the metastable minerals formed by alteration of the original parental rock that are present in the soil, as well as the slags themselves, have paramagnetic properties, while most of the soil components are diamagnetic; thus, a magnetic separation pretreatment (high-gradient magnetic field separation, for example) would be feasible [25,81].

4. Conclusions

The soil concentrations of potentially toxic elements were analyzed in five locations of the Linares mining district based on the geochemical background, the guideline levels established by Spanish legislation and the geoaccumulation criterion. The obtained results reveal anomalous soil concentrations in As, Cd, Cu, Pb, and Zn; in particular, As and Pb soil concentration exceeded the admissible limits in all the study sites and land-use scenarios considered. Moreover, the sequential soil extraction indicated that a significant proportion of these metal(loid)s (especially Pb) is present in bioavailable forms, thus posing a real threat to human health, as reflected in the risk assessment.

According to the information collected, remediation seems particularly promising by physical separation, which is particularly recommendable considering that most of the pollutants are concentrated in the fine grain size fraction (<63 μm), mainly in soil squares 12, 38, and 51. In this respect, we suggest gravity and even magnetic separation as complementary procedures attending to the nature of the minerals and waste found. Moreover, a second possibility is phytoremediation, which would be feasible as the available fractions of soil pollutants are significant. In this regard, a set of species for both phytoextraction and phytostabilization approaches are proposed.

Despite the potential advantages, these technologies are unlikely to achieve complete restoration of the sites as the natural ecosystem has been greatly disturbed by mining and metallurgy activities. Furthermore, we recommend the biomonitoring of potentially toxic elements in the study area in order to trace a possible introduction into the food chain. Authors expect that this research will serve as basis for future remediation to perform in the Linares mining district soils, which, as we have seen, is remarkable and affects a large surface of soils that could be refurbished for industrial or agricultural use.

Author Contributions: Conceptualization, C.S.; methodology, C.S. and J.M.; formal analysis, C.S.; investigation, C.S. and E.A.; resources, J.M. and J.R.; data curation, E.R.-V.; writing—original draft preparation, C.S., C.B., J.M. and E.R.-V.; writing—review and editing, I.M.H.R.A. and J.L.R.G.; visualization, C.B. and J.R.; supervision, J.L.R.G.; funding acquisition, J.L.R.G. and I.M.H.R.A. All authors have read and agreed to the published version of the manuscript.

Funding: This work was partially funded by the research projects NANOCAREM, MCI-20-PID2019-106939GB-I00 (AEI/Spain, FEDER/EU).

Acknowledgments: Carlos Boente obtained a postdoctoral contract within the PAIDI 2020 program (Ref 707 DOC 01097), cofinanced by the Junta de Andalucía (Andalusian Government). This work was developed under the project UIDB/04683/2020 and UIDP/04683/2020—ICT, Fundação para a Ciência e Tecnologia. The authors thank Noemi Esquinas for assistance provided with the sequential extraction procedures.

Conflicts of Interest: The authors declare no conflict of interest.

References

1. Kicińska, A. Environmental risk related to presence and mobility of As, Cd and Tl in soils in the vicinity of a metallurgical plant–Long-term observations. *Chemosphere* **2019**, *236*, 124308. [CrossRef] [PubMed]
2. Izydorczyk, G.; Mikula, K.; Skrzypczak, D.; Moustakas, K.; Witek-Krowiak, A.; Chojnacka, K. Potential environmental pollution from copper metallurgy and methods of management. *Environ. Res.* **2021**, *197*, 111050. [CrossRef] [PubMed]
3. Reyes, A.; Thiombane, M.; Panico, A.; Daniele, L.; Lima, A.; Di Bonito, M.; De Vivo, B. Source patterns of potentially toxic elements (PTEs) and mining activity contamination level in soils of Taltal city (northern Chile). *Environ. Geochem. Health* **2020**, *42*, 2573–2594. [CrossRef] [PubMed]
4. Gruszecka-Kosowska, A.; Kicińska, A. Long-Term Metal-Content Changes in Soils on the Olkusz Zn–Pb Ore-Bearing Area, Poland. *Int. J. Environ. Res.* **2017**, *11*, 359–376. [CrossRef]
5. Rapant, S.; Dietzová, Z.; Cicmanová, S. Environmental and health risk assessment in abandoned mining area, Zlata Idka, Slovakia. *Environ. Geol.* **2006**, *51*, 387–397. [CrossRef]
6. Wu, W.; Qu, S.; Nel, W.; Ji, J. The impact of natural weathering and mining on heavy metal accumulation in the karst areas of the Pearl River Basin, China. *Sci. Total Environ.* **2020**, *734*, 139480. [CrossRef]

7. Perlatti, F.; Martins, E.P.; de Oliveira, D.P.; Ruiz, F.; Asensio, V.; Rezende, C.F.; Otero, X.L.; Ferreira, T.O. Copper release from waste rocks in an abandoned mine (NE, Brazil) and its impacts on ecosystem environmental quality. *Chemosphere* **2021**, *262*, 127843. [CrossRef]
8. Gallego, J.R.; Esquinas, N.; Rodríguez-Valdés, E.; Menéndez-Aguado, J.M.; Sierra, C. Comprehensive waste characterization and organic pollution co-occurrence in a Hg and As mining and metallurgy brownfield. *J. Hazard. Mater.* **2015**, *300*, 561–571. [CrossRef]
9. Ali, H.; Khan, E.; Ilahi, I. Environmental Chemistry and Ecotoxicology of Hazardous Heavy Metals: Environmental Persistence, Toxicity, and Bioaccumulation. *J. Chem.* **2019**, *2019*, 1–14. [CrossRef]
10. Hogan, M.C. *Heavy Metal. Encyclopedia of Earth*; Monosson, E., Cleveland, C., Eds.; Heavy Meta: Washington, DC, USA, 2021.
11. Kabata-Pendias, A. *Trace Elements in Soils and Plants*; Routledge: London, UK, 2011; ISBN 9781420093681.
12. Gadd, G.M. Transformation and Mobilization of Metals, Metalloids, and Radionuclides by Microorganisms. In *Biophysico-Chemical Processes of Heavy Metals and Metalloids in Soil Environments*; Wiley: Hoboken, NJ, USA, 2007; pp. 53–96. ISBN 9780471737780.
13. Gál, J.; Hursthouse, A.; Cuthbert, S. Bioavailability of arsenic and antimony in soils from an abandoned mining area, Glendinning (SW Scotland). *J. Environ. Sci. Heal. Part* **2007**, *42*, 1263–1274. [CrossRef]
14. Rocco, C.; Seshadri, B.; Adamo, P.; Bolan, N.S.; Mbene, K.; Naidu, R. Impact of waste-derived organic and inorganic amendments on the mobility and bioavailability of arsenic and cadmium in alkaline and acid soils. *Environ. Sci. Pollut. Res.* **2018**, *25*, 25896–25905. [CrossRef]
15. Cerqueira, B.; Covelo, E.F.; Andrade, M.L.; Vega, F.A. Retention and Mobility of Copper and Lead in Soils as Influenced by Soil Horizon Properties. *Pedosphere* **2011**, *21*, 603–614. [CrossRef]
16. Borda, M.J.; Sparks, D.L. *Mobility of Trace Elements in Soil Environments*; Violante, A., Huang, P.M., Gadd, G.M., Eds.; John Wiley & Sons Inc.: Hoboken, NJ, USA, 2008.
17. US EPA. Risk Assessment Guidance for Superfund. Human Health Evaluation Manual Part A, Interim Final. *USA Environ. Prot. Agency* **1989**, *1*, 300.
18. US EPA. *Supplemental Guidance for Developing Soil Screening Levels for Superfund Sites*; U.S. Environmental Protection Agency: Washington, DC, USA, 2002; pp. 1–187.
19. Wuana, R.A.; Okieimen, F.E. Heavy Metals in Contaminated Soils: A Review of Sources, Chemistry, Risks and Best Available Strategies for Remediation. *ISRN Ecol.* **2011**, *2011*, 1–20. [CrossRef]
20. Yao, Z.; Li, J.; Xie, H.; Yu, C. Review on Remediation Technologies of Soil Contaminated by Heavy Metals. *Proc. Environ. Sci.* **2012**, *16*, 722–729. [CrossRef]
21. Boente, C.; Baragaño, D.; García-González, N.; Forján, R.; Colina, A.; Gallego, J.R. A holistic methodology to study geochemical and geomorphological control of the distribution of potentially toxic elements in soil. *Catena* **2022**, *208*, 105730. [CrossRef]
22. Sierra, C.; Martínez, J.; Menéndez-Aguado, J.M.; Afif, E.; Gallego, J.R. High intensity magnetic separation for the clean-up of a site polluted by lead metallurgy. *J. Hazard. Mater.* **2013**, *248–249*, 194–201. [CrossRef]
23. Sierra, C.; Menéndez-Aguado, J.M.; Afif, E.; Carrero, M.; Gallego, J.R. Feasibility study on the use of soil washing to remediate the As-Hg contamination at an ancient mining and metallurgy area. *J. Hazard. Mater.* **2011**, *196*, 93–100. [CrossRef]
24. Dermont, G.; Bergeron, M.; Mercier, G.; Richer-Lafleche, M. Soil washing for metal removal: A review of physical/chemical technologies and field applications. *J. Hazard. Mater.* **2008**, *152*, 1–31. [CrossRef]
25. Sierra, C.; Gallego, J.R.; Afif, E.; Menéndez-Aguado, J.M.; González-Coto, F. Analysis of soil washing effectiveness to remediate a brownfield polluted with pyrite ashes. *J. Hazard. Mater.* **2010**, *180*, 602–608. [CrossRef]
26. Boente, C.; Sierra, C.; Rodríguez-Valdés, E.; Menéndez-Aguado, J.M.; Gallego, J.R. Soil washing optimization by means of attributive analysis: Case study for the removal of potentially toxic elements from soil contaminated with pyrite ash. *J. Clean. Prod.* **2017**, *142*, 2693–2699. [CrossRef]
27. Wills, B.; Finch, J. *Mineral Processing Technology:An Introduction to the Practical Aspects of Ore Treatment and Mineral Recovery*; Elsevier: Amsterdam, The Netherlands, 2015; ISBN 0750644508.
28. Lee, J.H. An overview of phytoremediation as a potentially promising technology for environmental pollution control. *Biotechnol. Bioproc. Eng.* **2013**, *18*, 431–439. [CrossRef]
29. Khan, F.I.; Husain, T.; Hejazi, R. An overview and analysis of site remediation technologies. *J. Environ. Manag.* **2004**, *71*, 95–122. [CrossRef] [PubMed]
30. Lorestani, B.; Yousefi, N.; Cheraghi, M.; Farmany, A. Phytoextraction and phytostabilization potential of plants grown in the vicinity of heavy metal-contaminated soils: A case study at an industrial town site. *Environ. Monit. Assess.* **2013**, *185*, 10217–10223. [CrossRef] [PubMed]
31. Cheraghi, M.; Lorestani, B.; Khorasani, N.; Yousefi, N.; Karami, M. Findings on the phytoextraction and phytostabilization of soils contaminated with heavy metals. *Biol. Trace Elem. Res.* **2011**, *144*, 1133–1141. [CrossRef] [PubMed]
32. Vernon, R. The Linares lead mining district: The English connection. *Re Met.* **2009**, *13*, 1–10.
33. Arboledas Martínez, L. *Minería y Metalurgia Romana en el sur de la Península Ibérica: Sierra Morena Oriental*; Archaeopress: Oxford, UK, 2020.
34. Gutiérrez-Guzmán, F. *Las Minas de Linares: Apuntes Históricos*; El Colegio Oficial de Ingenieros Técnicos y Grados en Minas y Energía de Linares: Linares, Spain, 1999.

35. Azcárate, J.E. *Mapa Geológico y Memoria Explicativa de la Hoja 905, Escala 1:50*; Instituto Geológico y Minero de España: Madrid, Spain, 1977.
36. Lillo, J. Geology and Geochemistry of Linares-La Carolina Pb-Ore field (Southeastern border of the Hesperian Massif). Ph.D. Thesis, University of Leeds, Leeds, UK, 1992.
37. Lillo, J. Hydrothermal alteration in the Linares-La Carolina Ba-Pb-Zn-Cu-(Ag) vein district, Spain: Mineralogical data from El Cobre vein. *Trans. Inst. Min. Metall. Sect. Appl. Earth Sci.* **2002**, *111*, 114–118. [CrossRef]
38. Martínez López, J.; Llamas Borrajo, J.; De Miguel García, E.; Rey Arrans, J.; Hidalgo Estévez, M.C.; Sáez Castillo, A.J. Multivariate analysis of contamination in the mining district of Linares (Jaén, Spain). *Appl. Geochem.* **2008**, *23*, 2324–2336. [CrossRef]
39. Martínez, J. Caracterización Geoquímica y Ambiental de los Suelos en el Sector Minero de Linares. Ph.D. Thesis, University of Linares, Linares, Spain, 2002.
40. Martínez, J.; Rey, J.; Hidalgo, M.C.; Benavente, J. Characterizing abandoned mining dams by geophysical (ERI) and geochemical methods: The linares-la carolina district (Southern Spain). *Water Air. Soil Pollut.* **2012**, *223*, 2955–2968. [CrossRef]
41. Schulte, E.E.; Hopkins, B.G. Estimation of soil organic matter by weight loss-on-ignition. In *Soil Organic Matter: Analysis and Interpretation*; Wiley: Hoboken, NJ, USA, 2015; pp. 21–31. ISBN 9780891189411.
42. Klute, A. (Ed.) Nitrogen-total. In *Methods of Soil Analyses*; Soil Science Society of America: Madison, WI, USA, 1996; pp. 595–624.
43. Mehlich, A. Mehlich 3 Soil Test Extractant: A Modification of Mehlich 2 Extractant. *Commun. Soil Sci. Plant Anal.* **1984**, *15*, 1409–1416. [CrossRef]
44. Monterroso, C.; Álvarez, E.; Marcos, M.L. Evaluation of Mehilich 3 reagent as a multielement extractant in mine soils. *Land Degrad. Dev.* **1999**, *10*, 35–47. [CrossRef]
45. Pansu, M.; Gautheyrou, J. *Handbook of Soil Analysis: Mineralogical, Organic and Inorganic Methods*; Springer: Berlin/Heidelberg, Germany, 2006; ISBN 9783540312116.
46. Gee, G.W.; Bauder, J.W. Particle-size analysis. In *Methods of Soil Analysis, Part 1: Physical and Mineralogical Methods*; Wiley: Hoboken, NJ, USA, 2018; pp. 383–411. ISBN 9780891188643.
47. Müller, G. Index of geoaccumulation in sediments of the Rhine River. *Geol. J.* **1969**, *2*, 108–118.
48. Ure, A.M.; Quevauviller, P.; Muntau, H.; Griepink, B. Speciation of heavy metal in soils and sediments. An account ofthe improvement and harmonisation of extraction techniques undertaken under the auspices of the BCR of the Commission of the European Communities. *Int. J. Environ. Anal. Chem.* **1993**, *51*, 135–152. [CrossRef]
49. ISO Soil Quality. *Extraction of Trace elements Soluble in Aqua Regia*; ISO 114661995(E); ISO: Geneva, Switzerland, 1995.
50. Pueyo, M.; Mateu, J.; Rigol, A.; Vidal, M.; López-Sánchez, J.F.; Rauret, G. Use of the modified BCR three-step sequential extraction procedure for the study of trace element dynamics in contaminated soils. *Environ. Pollut.* **2008**, *152*, 330–341. [CrossRef] [PubMed]
51. Larios, R.; Fernández-Martínez, R.; Rucandio, I. Comparison of three sequential extraction procedures for fractionation of arsenic from highly polluted mining sediments. *Anal. Bioanal. Chem.* **2012**, *402*, 2909–2921. [CrossRef]
52. Zhao, S.; Feng, C.; Yang, Y.; Niu, J.; Shen, Z. Risk assessment of sedimentary metals in the Yangtze Estuary: New evidence of the relationships between two typical index methods. *J. Hazard. Mater.* **2012**, *241–242*, 164–172. [CrossRef]
53. BOE Real Decreto 9/2005 por el que se establece la relación de actividades potencialmente contaminantes del suelo y los criterios y estándares para la declaración de suelos contaminados. *Gov. Spain* **2005**, *15*, 1833–1843.
54. Carlon, C. *Derivation Methods of Soil Screening Values in Europe. a Review and Evaluation of National Procedures towards Harmonisation*; Office for Official Publications of the European Communities: Luxembourg, 2007; ISBN 9789279052385.
55. Gil-Díaz, M.; Alonso, J.; Rodríguez-Valdés, E.; Pinilla, P.; Lobo, M.C. Reducing the mobility of arsenic in brownfield soil using stabilised zero-valent iron nanoparticles. *J. Environ. Sci. Health. Tox. Hazard. Subst. Environ. Eng.* **2014**, *49*, 1361–1369. [CrossRef]
56. US EPA. Revised Interim Soil Lead Guidance for CERCLA Sites and RCRA Corrective Action Facilities. *OSWER Dir.* **1994**, *9355*, 4–12.
57. Zagorodni, A.A. *Ion Exchange Materials: Properties and Applications*; Elsevier: Amsterdam, The Netherlands, 2007; ISBN 9780080445526.
58. Martínez, J.; Llamas, J.F.; De Miguel, E.; Rey, J.; Hidalgo, M.C.; Sáez-Castillo, A.J. Determination of geochemical back ground in a metal mining site: Example of the mining district of Linares (south Spain). *J. Geochem. Explor.* **2007**, *94*, 19–29. [CrossRef]
59. Ottonello, G. *Principles of Geochemistry*; Columbia University Press: New York, NY, USA, 2000.
60. Sponza, D.; Karaoglu, N. Environmental geochemistry and pollution studies of Aliaga metal industry district. *Environ. Int.* **2002**, *27*, 541–553. [CrossRef]
61. Alloway, B.J. *Heavy Metals in Soils*; Springer: Berlin/Heidelberg, Germany, 2013; ISBN 978-94-010-4586-5.
62. Antunes, M.; Santos, A.; Valente, T.; Albuquerque, T. Spatial Mobility of U and Th in a U-enriched Area (Central Portugal). *Appl. Sci.* **2020**, *10*, 7866. [CrossRef]
63. Boente, C.; Gerassis, S.; Albuquerque, M.T.D.; Taboada, J.; Gallego, J.R. Local versus Regional Soil Screening Levels to Identify Potentially Polluted Areas. *Math. Geosci.* **2020**, *52*, 381–396. [CrossRef]
64. Bartholomew, C.J.; Li, N.; Li, Y.; Dai, W.; Nibagwire, D.; Guo, T. Characteristics and health risk assessment of heavy metals in street dust for children in Jinhua, China. *Environ. Sci. Pollut. Res.* **2020**, *27*, 5042–5055. [CrossRef] [PubMed]
65. Zhong, M.; Jiang, L. Refining health risk assessment by incorporating site-specific background concentration and bioaccessibility data of Nickel in soil. *Sci. Total Environ.* **2017**, *581–582*, 866–873. [CrossRef]

66. Boente, C.; Albuquerque, M.T.D.; Gallego, J.R.; Pawlowsky-Glahn, V.; Egozcue, J.J. Compositional baseline assessments to address soil pollution: An application in Langreo, Spain. *Sci. Total Environ.* **2022**, *812*, 152383. [CrossRef]
67. Filgueiras, A.V.; Lavilla, I.; Bendicho, C. Chemical sequential extraction for metal partitioning in environmental solid samples. *J. Environ. Monit.* **2002**, *4*, 823–857. [CrossRef]
68. Saleem, M.; Iqbal, J.; Shah, M.H. Geochemical speciation, anthropogenic contamination, risk assessment and source identification of selected metals in freshwater sediments—A case study from Mangla Lake, Pakistan. *Environ. Nanotechnol. Monit. Manag.* **2015**, *4*, 27–36. [CrossRef]
69. Yang, Z.; Wang, Y.; Shen, Z.; Niu, J.; Tang, Z. Distribution and speciation of heavy metals in sediments from the mainstream, tributaries, and lakes of the Yangtze River catchment of Wuhan, China. *J. Hazard. Mater.* **2009**, *166*, 1186–1194. [CrossRef]
70. Li, Y.; Hu, J.; Wu, W.; Liu, S.; Li, M.; Yao, N.; Chen, J.; Ye, L.; Wang, Q.; Zhou, Y. Application of IEUBK model in lead risk assessment of children aged 61–84 months old in central China. *Sci. Total Environ.* **2016**, *541*, 673–682. [CrossRef]
71. Dean, J.R.; Elom, N.I.; Entwistle, J.A. Use of simulated epithelial lung fluid in assessing the human health risk of Pb in urban street dust. *Sci. Total Environ.* **2017**, *579*, 387–395. [CrossRef] [PubMed]
72. Triantafyllidou, S.; Le, T.; Gallagher, D.; Edwards, M. Reduced risk estimations after remediation of lead (Pb) in drinking water at two US school districts. *Sci. Total Environ.* **2014**, *466–467*, 1011–1021. [CrossRef] [PubMed]
73. Bolan, N.; Kunhikrishnan, A.; Thangarajan, R.; Kumpiene, J.; Park, J.; Makino, T.; Kirkham, M.B.; Scheckel, K. Remediation of heavy metal(loid)s contaminated soils-To mobilize or to immobilize? *J. Hazard. Mater.* **2014**, *266*, 141–166. [CrossRef] [PubMed]
74. Radziemska, M.; Bęś, A.; Gusiatin, Z.M.; Cerdà, A.; Jeznach, J.; Mazur, Z.; Brtnický, M. Assisted phytostabilization of soil from a former military area with mineral amendments. *Ecotoxicol. Environ. Saf.* **2020**, *188*, 109934. [CrossRef]
75. Rosario, K.; Iverson, S.L.; Henderson, D.A.; Chartrand, S.; McKeon, C.; Glenn, E.P.; Maier, R.M. Bacterial Community Changes during Plant Establishment at the San Pedro River Mine Tailings Site. *J. Environ. Qual.* **2007**, *36*, 1249–1259. [CrossRef]
76. Jefferson, L.V. Implications of plant density on the resulting community structure of mine site land. *Restor. Ecol.* **2004**, *12*, 429–438. [CrossRef]
77. Mendez, M.O.; Maier, R.M. Phytostabilization of mine tailings in arid and semiarid environments-An emerging remediation technology. *Environ. Health Perspect.* **2008**, *116*, 278–283. [CrossRef]
78. Del Río-Celestino, M.; Font, R.; Moreno-Rojas, R.; De Haro-Bailón, A. Uptake of lead and zinc by wild plants growing on contaminated soils. *Ind. Crops Prod.* **2006**, *24*, 230–237. [CrossRef]
79. Conesa, H.M.; Faz, Á.; Arnaldos, R. Heavy metal accumulation and tolerance in plants from mine tailings of the semiarid Cartagena-La Unión mining district (SE Spain). *Sci. Total Environ.* **2006**, *366*, 1–11. [CrossRef]
80. Conesa, H.M.; Robinson, B.H.; Schulin, R.; Nowack, B. Growth of Lygeum spartum in acid mine tailings: Response of plants developed from seedlings, rhizomes and at field conditions. *Environ. Pollut.* **2007**, *145*, 700–707. [CrossRef]
81. Sierra, C.; Boado, C.; Saavedra, A.; Ordóñez, C.; Gallego, J.R. Origin, patterns and anthropogenic accumulation of potentially toxic elements (PTEs) in surface sediments of the Avilés estuary (Asturias, northern Spain). *Mar. Pollut. Bull.* **2014**, *86*, 530–538. [CrossRef] [PubMed]